Available online at www.sciencedirect.com

ScienceDirect

www.elsevier.com/locate/jes

JES JOURNAL OF ENVIRONMENTAL SCIENCES

www.jesc.ac.cn

Research Article

Unexpected/contrary behavior of aerosol mass concentration in response to the individual components' concentration reduction in Kitakyushu, Japan

Xi Zhang[1,2], *Takuya Murakami*[1], *Jinhe Wang*[2], *Masahide Aikawa*[1,*]

[1] *Faculty of Environmental Engineering, The University of Kitakyushu, 1-1, Hibikino, Wakamatsu, Kitakyushu, Fukuoka 808-0135, Japan*

[2] *Resources and Environment Innovation Research Institute, School of Municipal and Environmental Engineering, Shandong Jianzhu University, Jinan 250101, China*

ARTICLE INFO

Article history:
Received 28 January 2022
Revised 25 August 2022
Accepted 17 September 2022
Available online 28 September 2022

Keywords:
Sensitive tests
Reduction
Gas-particle conversion process
Aerosol liquid water content
Sea salts

ABSTRACT

In the suburbs of Kitakyushu, Japan, the inorganic aerosol mass concentration (IAM) was about 32.7 μg/m^3, with the aerosol pH of 3.3. To study the thermodynamics of aerosol when its individual components' concentration is reduced, sensitive tests were performed using the ISORROPIA II model, in which the seven control species—TNaCl, TNH_4^+, TSO_4^{2-}, TNO_3^-, TMg^{2+}, TK^+, and TCa^{2+}—were taken into account. IAM and inorganic aerosol pH after reducing TNaCl, TNO_3^-, TMg^{2+}, TK^+, and TCa^{2+} responded linearly (0% ≤ concentration reduction ratio (CRR) ≤ 100%, with the exception of 100% in TNaCl); the nonlinear variations of these two parameters could be observed by controlling TNH_4^+ and TSO_4^{2-}. Unexpected aerosol behavior occurred at 100% reduction of TNaCl, which was caused by the sudden increase of NO_3^-, NH_4^+, and aerosol liquid water content (ALWC); the increase of IAM was also observed after controlling TSO_4^{2-} (60% ≤ CRR ≤ 100%) and TCa^{2+} (0% ≤ CRR ≤ 100%), which was mainly related to the variation of ALWC driven by the response of $CaSO_4$. Multiple regression analysis showed that ALWC was statistically and strongly related to the variations of NO_3^-, Cl^-, SO_4^{2-}, HSO_4^-, HNO_3, and NH_3 ($P < 0.05$), with regression coefficients of 1.68, 5.23, 1.83, 2.81, 0.34, and 0.57, respectively. The highest coefficient (5.23) was found for Cl^-, revealing that sea salts significantly influenced particle responses. Overall, this study comprehensively investigated aerosol characteristics and inner responses for the reduction of components, which is of great significance for a better understanding of atmospheric chemistry in Kitakyushu, Japan.

* Corresponding author.
E-mail: masahide_aikawa@kitakyu-u.ac.jp (M. Aikawa).

https://doi.org/10.1016/j.jes.2022.09.024
1001-0742/

Introduction

Atmospheric inorganic aerosols are complex mixtures that originate from various pollution sources and have different formation pathways, basically accounting for one third or more of total particulate matters, and main components are sea salts, secondary inorganic ions, crustal materials, and liquid water (Khan et al., 2010; Kong et al., 2018; Yin et al., 2018; Ng et al., 2019; Roig Rodelas et al., 2019; Zhang et al., 2020, 2021b). The related environmental problems include air quality deterioration, human health risk, climate change, visibility reduction, etc., which are closely related to the loading level of inorganic aerosols in the atmosphere and the physical/chemical characteristics of components (Xue et al., 2011; Carnevale et al., 2012; Tan et al., 2017; Gao et al., 2020). To improve air quality, strict standards for atmospheric particles have been established by individual governments and international organizations (Chen et al., 2016; Wang et al., 2018; Roberts and Wooster, 2021; Zhang et al., 2021a). Controlling particle mass concentration level is necessary and urgent to achieve these environmental standards, especially in the severe pollution regions; moreover, the effective countermeasures are required based on the specific situations of different regions or countries. In previous studies, the thermodynamic inorganic model, ISORROPIA II, was often used to simulate the gas-particle conversion process, providing a simple and effective method of predicting inorganic aerosol behavior. To be specific, San et al. (2005) modeled the response of inorganic aerosols to changes in sulfate, nitrate, and ammonium concentrations (SNA) in Mexico City; the results indicated that particle behavior was dominated by the abundance of ammonia, and changes in sulfate and nitrate concentrations were expected to have a greater effect on IAM in an ammonium-rich condition. Zhang et al. (2020) observed that when the atmosphere had an ammonium-rich condition, the reduction of nitrate emissions was the optimal control measure for fine particle pollution in urban Beijing, followed by controlling sulfate and ammonium concentrations. Ansari and Pandis (1998) simulated the 20% reduction of SNA in two polluted urban areas, showing that reductions in ammonia emissions had the most significant impact on the total particle concentration level in ammonium-poor conditions, although such a reduction would substantially increase atmospheric acidity. Walker et al. (2006) used the same approach to assess the effect of a 50% reduction, clearly illustrating that inorganic fine particles were most sensitive to a reduction in sulfate concentration during warm months and approximately equally sensitive to reductions in sulfate and nitrate concentrations during cold months. It should be noted that these studies focused on the effects of changes in SNA concentrations but not the effects of changes in the amounts of NH_3, SO_2, and NOx emissions on the ambient air quality; moreover, ALWC was the sensitive component, showing its relatively high contribution for the variation of IAM (Zhang et al., 2022).

In the present study, year-round observation of atmospheric particles and gaseous pollutants (HNO_3, HCl, and NH_3) was carried out in the suburbs of western Japan using a four-stage filter-pack method (Aikawa et al., 2013; 2016). Combining with these field observation data, the sensitive tests for different aerosol components were performed by means of ISORROPIA II model. The main objective was to comprehensively assess how inorganic aerosols respond to concentration reducing of components, to investigate their deep mechanisms and the characteristics of sensitive aerosol components, and, as a consequence, to provide a better understanding of the chemistry of particles in the suburbs of Kitakyushu, Japan, and further to throw out a methodology widely applicable for a deeper comprehension of the atmospheric chemistry.

1. Materials and methods

1.1. *Sampling and chemical analysis*

Air sampling was conducted on the roof of the North Building, Hibikino Campus, the University of Kitakyushu (33.89° N, 130.71° E). This sampling site is in a suburb of Kitakyushu City, being ca. 15 km from the central part of the city, as illustrated in Fig. 1. The four-stage filter-pack method was used to collect total particulate matter (TPM) and gaseous pollutants (SO_2, HNO_3, HCl, and NH_3) simultaneously. The samples were collected on a daily (noon-noon) basis from March 2017 to February 2018. The procedure for determining water-soluble ions (Na^+, NH_4^+, K^+, Mg^{2+}, Ca^{2+}, Cl^-, NO_3^-, and SO_4^{2-}) was described in detail in previous studies (Aikawa et al., 2005, 2010, 2013, 2016, 2017a), and ion chromatography (Thermo Scientific™ Dionex™ Integrion, Thermo Fisher Scientific Inc., Waltham, MA, USA) was used in the determination. More detailed information about the sampling site, experiment methodology, and the process of quality assurance and quality control was shown in our previous publication (Zhang et al., 2021b).

1.2. *Model calculation*

The thermodynamic equilibrium models (ISORROPIA, E-AIM, GFEMN, HETV, MESA and UHAERO) are widely used for investigating the gas-particle conversion process of inorganic aerosols; however, an important limitation of these models is the lack of treatment of crustal species (Ca^{2+}, K^+, and Mg^{2+}) (Karydis et al., 2010). To improve the simulation accuracy, Fountoukis and Nenes (2007) introduced a new thermodynamic model, ISORROPIA II, in which the thermodynamics of the crustal species have been added to the preexisting suite of components of the ISORROPIA model; many studies have adopted this new model to analyze the characteristics of coarse particles (Quan and Zhang, 2008; Karydis et al., 2010; Xue et al., 2011; Carnevale et al., 2012).

In this study, the ISORROPIA II model was run in the forward mode with input data of relative humidity (RH), temperature (T), and the concentrations of sodium (Na^+), chloride ($HCl + Cl^-$), ammonium ($NH_3 + NH_4^+$), sulfate (SO_4^{2-}), nitrate ($HNO_3 + NO_3^-$), magnesium (Mg^{2+}), potassium (K^+), calcium (Ca^{2+}) (abbreviated as TNa^+, TCl^-, TNH_4^+, TSO_4^{2-}, TNO_3^-, TMg^{2+}, TK^+, and TCa^{2+} hereafter) (Sudheer et al., 2015; Kong et al., 2018; Wang et al., 2019; Zhang et al., 2020, 2021b). Then, the stable state or metastable state was selected for

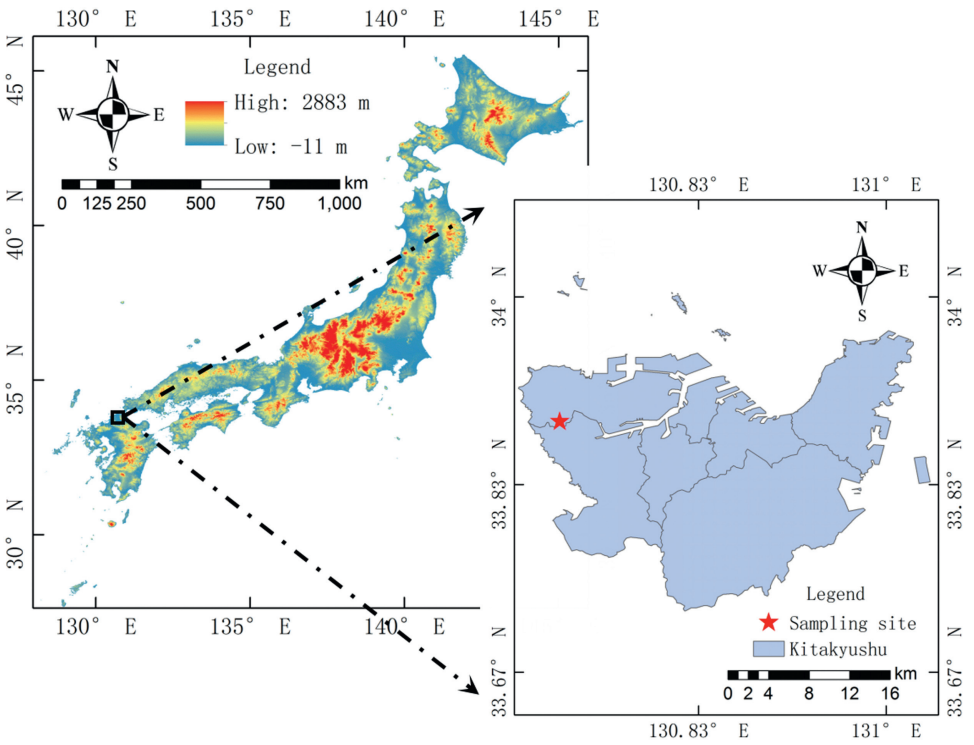

Fig. 1 – Location of sampling site.

inorganic aerosols based on the specific condition of sampling site. For stable condition, salts precipitate once the aqueous phase becomes saturated with respect to a salt, while, for metastable condition, the aerosol is composed only of an aqueous phase regardless of its saturation state (Xue et al., 2011). Finally, this model predicted which species can exist in the gas phase, aerosol solid phase, and aerosol aqueous phase, and calculated their concentration levels at chemical equilibrium, as well as aerosol pH.

2. Results and discussion

2.1. *Simulation quality of the ISORROPIA II model*

To assess the simulation quality of the ISORROPIA II model, the output data of NH_4^+, NO_3^-, and Cl^- in the aerosol phase and NH_3, HNO_3, and HCl in the gas phase were compared with data observed by the four-stage filter-pack method using four statistical parameters, including mean bias (MB), mean error (ME), normalized mean bias (NMB), and normalized mean error (NME) (Karydis et al., 2010; Li et al., 2015; Li et al., 2017a; Sudheer et al., 2015; Zhang et al., 2017; Chen et al., 2018). The statistical analysis of the agreement between observations and model predictions in stable and metastable conditions is shown in Table 1. The values of these four parameters in a metastable state were closer to 0 than those in a stable state, which reveals that the metastable condition was the more suitable atmospheric situation in the suburbs of western Japan. In addition, NH_4^+, Cl^-, and HNO_3 showed negative values of MB and NMB under metastable condition, which indicates that the simulation results slightly underestimate these three species and overestimate NH_3, HCl, and NO_3^-. However, in total, the simulation bias in this study was still within acceptable levels (Karydis et al., 2010; Sudheer et al., 2015). Moreover, the ALWC derived from two different thermodynamic models (ISORROPIA II and E-AIM III) agreed well, with an R^2 value of 0.97 and a slope of 1.00 (Zhang et al., 2021b). Thus, the simulation results of the ISORROPIA II model in metastable conditions were reliable and can be applicable to the following analysis.

2.2. *Original atmospheric condition (base case)*

Table 2 shows the initial atmospheric situation in Kitakyushu City, Japan, as simulated by the ISORROPIA II model, which served as the base case for the seven sensitive tests. Specifically, the average mass concentrations of three gaseous pollutants (NH_3, HCl, and HNO_3) were 1.8, 1.1, and 1.1 μg/m^3, respectively, and the IAM was about 32.7 μg/m^3, with the aerosol pH of 3.3. Among the inorganic aerosol components, only $CaSO_4$ was in an aerosol solid phase, with an average concentration of 2.4 μg/m^3, while other components, including Na^+, Cl^-, NH_4^+, SO_4^{2-}, NO_3^-, K^+, Mg^{2+}, and ALWC, were all in aerosol aqueous phase, and the concentrations were 1.5, 1.6, 1.4, 3.1, 3.2, 0.2, 0.2, and 19.2 μg/m^3, respectively.

The high loading of the ALWC revealed that inorganic aerosols were highly humid, playing an important role in both visibility impairment and aerosol radiative forcing (Xue et al., 2011). Many studies have proved that the ALWC was principally influenced by the relative humidity (Tan et al., 2017; Xu et al., 2017; Wu et al., 2018; Wang et al., 2019; Huang et al., 2021), which was consistent with our result. From Fig. 2(a), it can be seen that the ALWC increased exponentially with the

Table 1 – Statistical evaluation of the simulation results of the ISORROPIA II model.

Species	MB (μg/m³)		ME (μg/m³)		NMB (%)		NME (%)	
	Stable	Metastable	Stable	Metastable	Stable	Metastable	Stable	Metastable
NH_4^+	−0.43	−0.34	0.55	0.48	−26.14	−27.75	33.76	39.15
Cl^-	−0.36	−0.28	0.51	0.45	−19.23	−18.23	27.20	29.44
NO_3^-	−0.18	0.02	0.76	0.62	−5.46	0.68	23.43	20.36
NH_3	0.43	0.34	0.55	0.48	29.94	18.08	38.65	25.50
HCl	0.36	0.28	0.51	0.45	45.71	24.02	64.71	38.82
HNO_3	0.18	−0.02	0.76	0.62	15.30	−1.51	65.36	46.58

Note: $MB = \frac{1}{N} \times \sum_{i=1}^{N} (S_i - O_i)$; $ME = \frac{1}{N} \times \sum_{i=1}^{N} |S_i - O_i|$; $NMB = \frac{\sum_{i=1}^{N} (S_i - O_i)}{\sum_{i=1}^{N} O_i} \times 100\%$; $NME = \frac{\sum_{i=1}^{N} |S_i - O_i|}{\sum_{i=1}^{N} O_i} \times 100\%$; where S_i is the simulated value of the pollutant concentration, O_i is the observed value of the corresponding pollutant concentration at the same time, and N is the total number of the samples (365).

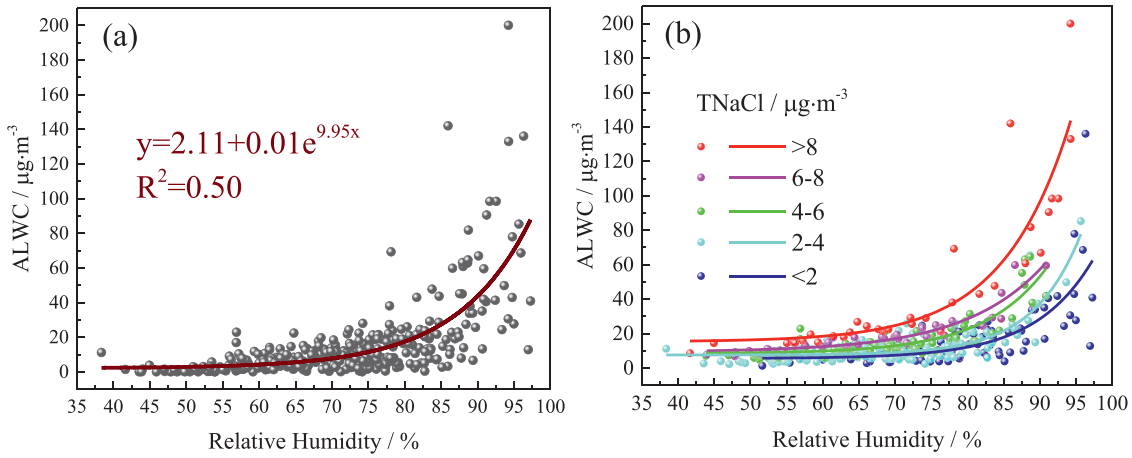

Fig. 2 – Variation of the ALWC as a function of the relative humidity (a), and the further influence of marine aerosols on the ALWC (b). The samples are grouped according to the concentration level of TNaCl in the atmosphere in Fig. 2 (b).

Table 2 – The simulated concentrations of related species in the gas phase and the aerosol phase by ISORROPIA II.

Phase	Species	Mean value (μg/m³)
Gas phase	NH_3	1.8
	HNO_3	1.1
	HCl	1.1
Aerosol solid phase	$CaSO_4$	2.4
Aerosol aqueous phase	Na^+	1.5
	Cl^-	1.6
	NH_4^+	1.4
	SO_4^{2-}	3.1
	HSO_4^-	0.0
	NO_3^-	3.2
	K^+	0.2
	Mg^{2+}	0.2
	Ca^{2+}	0.0
	ALWC	19.2

Note: The initial input data (mean value): RH (70%), T (289.9 K), TNa^+ (1.5 μg/m³), TCl^- (2.7 μg/m³), TNH_4^+ (3.1 μg/m³), TSO_4^{2-} (4.9 μg/m³), TNO_3^- (4.4 μg/m³), TK^+ (0.2 μg/m³), TMg^{2+} (0.2 μg/m³), and TCa^{2+} (0.8 μg/m³).

increase of the relative humidity. When the relative humidity was lower than 60%, the concentration of aerosol liquid water was approximately 2.11 μg/m³ and basically was unchanged, which was because the hygroscopic effect of atmospheric particles was minimal under low-humidity conditions, and the moisture level was too low to be absorbed effectively by particles (Tan et al., 2017). In contrast, when the ambient RH increased from 60% to 85%, the ALWC increased gradually, and this gradual increase could be attributable to the absorption of water by mixed deliquescent salts. Fong et al. (2016) and Wu et al. (2018) actually demonstrated that when the ambient RH reached the lowest deliquescence relative humidity (DRH) of inorganic salts in aerosols (Li et al., 2017b), with increased RH, more and more inorganic salts absorbed water to form saturated solution droplets, until the aerosol system fully deliquesced. Finally, when the relative humidity exceeded approximately 85%, water molecules in the atmosphere started to be adsorbed on aerosol surfaces, forming a water layer, and the thickness of the water layer increased quickly with the humidity (He et al., 2019), causing the obviously higher rate of increase of ALWC.

2.3. *Thermodynamic equilibrium shifts of particle-related species in seven sensitive tests*

2.3.1. *Response to the reduction in TNaCl concentration*

In the suburbs of western Japan, TNa^+ and TCl^- are mainly from marine aerosols, and their atmospheric concentrations are easy to vary synchronously with changes in the propor-

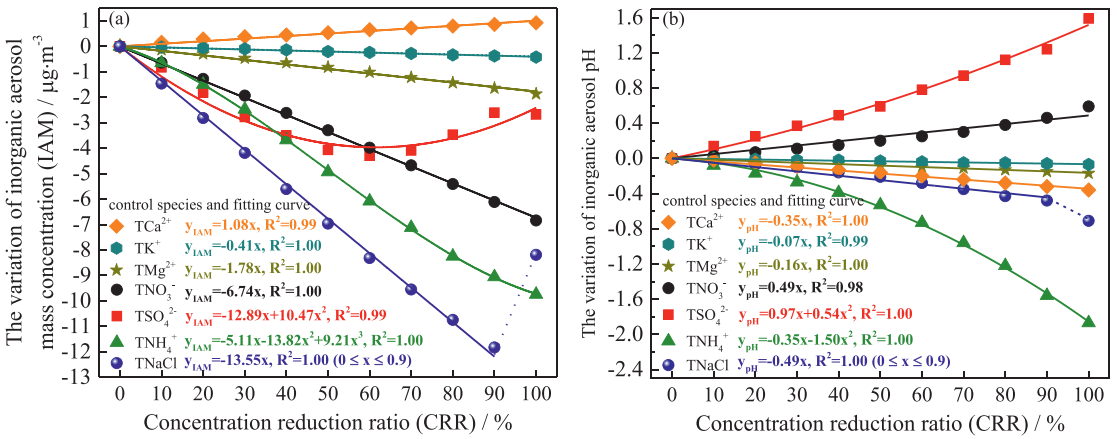

Fig. 3 – Variations of inorganic aerosol mass concentrations (a) and pH (b) in seven sensitive tests (CRR=$\frac{C_0-C_1}{C_0}$ × 100%, where C_0 and C_1 represent species concentrations in cases of without reduction and with reduction, respectively.).

tion and transport speed of air masses from the Sea of Japan (Aikawa et al., 2017b; 2018; Zhang et al., 2021b). Considering the condition in different influence of marine aerosol, the responses of IAM and aerosol pH for different TNaCl ($Na^+ + HCl + Cl^-$) condition were simulated in this study. As shown in Fig. 3(a), when TNaCl in the atmosphere decreased from 4.2 μg/m^3 (0% reduction) to 0.4 μg/m^3 (90% reduction), the IAM responded linearly with a slope of -13.55, and its concentration variation was obviously higher than those of the other six sensitive tests. During the corresponding gas-particle conversion process (Fig. 4(a)), the ALWC was the most sensitive component in the aerosol phase, which could explain approximately 72% of the total particle concentration variation, followed by the sum of Na^+ and Cl^- (23%). This phenomenon revealed that the concentration level of marine aerosols could also affect the ALWC, except for the relative humidity. A more-detailed analysis regarding factors involved in the ALWC is shown in the following Section 2.3.4. In addition, the slight drop in NO_3^- concentration was mainly due to the thermodynamic equilibrium shift of aged sea salts from an aerosol aqueous phase ($NaNO_3$) to a gas phase (HNO_3) (Boreddy and Kawamura, 2016; Ge et al., 2017). Under the influence of these four particle components (ALWC, Na^-, Cl^-, and NO_3^-), the inorganic aerosol pH after controlling TNaCl was obviously lower than that in base case, and its response followed the linear variation with the slope of -0.49 (Fig. 3(b)). Previous researches have shown that low pH could activate particle-bound hazardous materials (e.g., trace metals); hence, the response of inorganic aerosol pH after controlling TNaCl could cause the aggravation of human health risk to a certain extent (Kong et al., 2018; Zhang et al., 2019; Gao et al., 2020; Song and Osada, 2021). However, when the CRR of TNaCl was 100%, the IAM increased by 3.6 μg/m^3, and aerosol pH decreased at a larger rate than before. To understand this sudden change, we simulated the gas-particle conversion processes in detail for 91%, 92%, 93%, 94%, 95%, 96%, 97%, 98%, and 99% reductions of TNaCl (Fig. 4(b)). Fig. 4(b) indicated that the responses of inorganic aerosols in conditions of 91%–99% reduction followed the original equation. The sharp variation in the IAM was only observed at 100% reduction, which was due to the changes of NO_3^-, NH_4^+, and ALWC in the aerosol aqueous phase. The conversion process of nitrate and ammonium from the gas phase to the aerosol aqueous phase could be enhanced effectively with the extremely low concentration of marine aerosols; this subsequently influenced the concentration level of the ALWC, finally resulting in the increase of the IAM and aerosol acidity.

2.3.2. *Individual response to the reduction for TNH_4^+, TSO_4^{2-}, and TNO_3^- concentrations*

As opposed to marine aerosols from natural sources, secondary inorganic aerosols are mainly from anthropogenic sources and play a dominant role in severe particle pollution (Sun et al., 2016; Roig Rodelas et al., 2019; Xu et al., 2019; Zhang et al., 2020). When we reduced TNH_4^+ and TSO_4^{2-} concentrations, the IAM and inorganic aerosol pH changed nonlinearly (the fitting curves: $y_{IAM} = -5.11x - 13.82x^2 + 9.21x^3$, $y_{pH} = -0.35x - 1.50x^2$, and $y_{IAM} = -12.89x + 10.47x^2$, $y_{pH} = 0.97x + 0.54x^2$, respectively (y_{IAM}, y_{pH}, and x presents IAM variation [μg/m^3], inorganic aerosol pH variation [dimensionless], and CRR/100 [dimensionless]); only controlling TNO_3^- showed the linear aerosol responses, with the slope of -6.74 for IAM, and of 0.49 for pH (Fig. 3).

To better understand the aerosol behaviors in these three sensitive tests, the variations of related species in the gas phase, aerosol solid phase, and aerosol aqueous phase were further investigated. From Fig. 4(c), it can be seen that after reducing the concentration of TNH_4^+, NH_3 in the gas phase and NH_4^+ in the aerosol aqueous phase decreased simultaneously. With this reducing NH_4^+, the Cl^- and NO_3^-, which had combined with this reduced NH_4^+ (NH_4Cl and NH_4NO_3), were continuously released into the atmosphere in the gaseous form; hence, the concentrations of HCl and HNO_3 in the gas phase increased obviously. In addition, when the CRR of TNH_4^+ was larger than 60%, the remaining NH_4^+ in the aerosol phase was lower than 0.9 μg/m^3, which was not sufficient for maintaining all SO_4^{2-} with the chemical form of $(NH_4)_2SO_4$; hence, the appearance of HSO_4^- was observed in the aerosol aqueous phase. During the entire process, the ALWC was the most sensitive component, accounting for ca. 64% of the IAM varia-

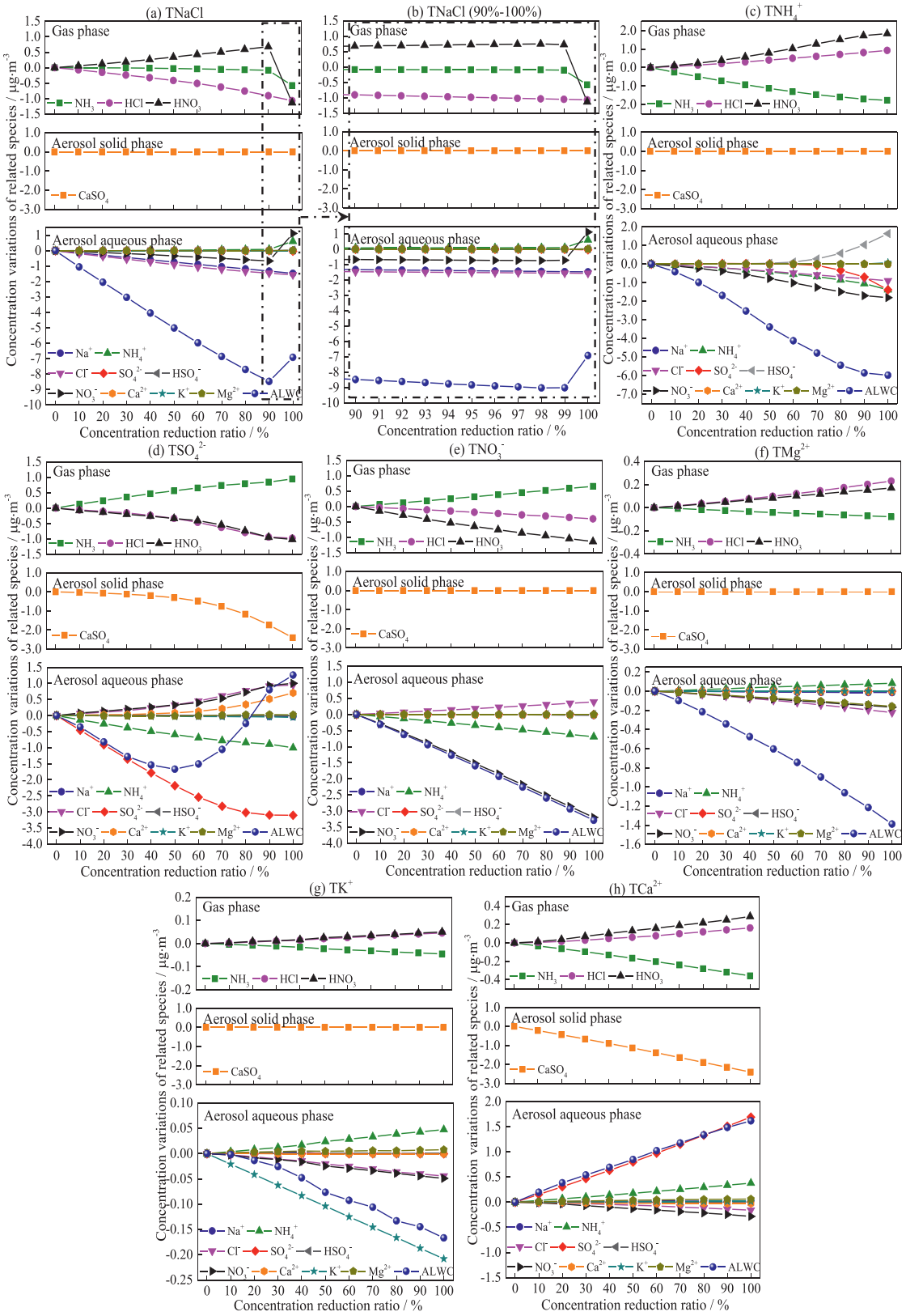

Fig. 4 – Concentration variations of related species in the gas phase and the aerosol phase in seven sensitive tests.

tion. Finally, under the comprehensive influence of NH_4^+, Cl^-, NO_3^-, SO_4^{2-}, HSO_4^-, and ALWC, the inorganic aerosol pH decreased nonlinearly in the strict sense, and the lowest value (1.4) was observed under 100% reduction of TNH_4^+ (Fig. 3(b)).

Different with controlling TNH_4^+, when the TSO_4^{2-} decreased from 4.9 (0% reduction) to 2.5 μg/m^3 (50% reduction), the concentration of SO_4^{2-} in the aerosol aqueous phase obviously decreased, while the concentration of $CaSO_4$ in the aerosol solid phase had little change (Fig. 4(d)). For NH_4^+ that was bound to these reduced SO_4^{2-}, one part could be directly released into the atmosphere, causing the increase of NH_3 in the gas phase, and the other part could be combined with the Cl^- and NO_3^-, which were transformed from gaseous HCl and HNO_3. When the CRR of TSO_4^{2-} exceeded 50%, $CaSO_4$ also started to decrease significantly, and most of the Ca^{2+} in the aerosol solid phase could enter the aerosol aqueous phase. In addition, during the entire process, the variation of the ALWC was obviously different from that of other components; that is, the ALWC gradually decreased as TSO_4^{2-} decreased, and the amount of the decreased ALWC became smaller and smaller when the CRR was larger than 50%. Totally speaking, the variation of the IAM was mainly determined by the concentration variations of SO_4^{2-} and ALWC in the aerosol aqueous phase, and 60% reduction in TSO_4^{2-} resulted in the largest decrease (4.3 μg/m^3). In addition, among seven sensitive tests, controlling TSO_4^{2-} concentration was the most effective to decrease aerosol acidity (Fig. 3).

As for controlling TNO_3^- (Fig. 4(e)), NO_3^- in the aerosol aqueous phase and HNO_3 in the gas phase decreased simultaneously. Subsequently, most of NH_4^+ bound to the reduced NO_3^- was directly released into the atmosphere, causing a linear increase of NH_3 in the gas phase, and a small part of NH_4^+ was combined with Cl^-, which was transformed from gaseous HCl. During this gas-particle conversion process, the ALWC decreased linearly with a slope of -3.2. Finally, the aerosol pH obviously increased under the comprehensive influence of Cl^-, NH_4^+, NO_3^-, and ALWC in the aerosol aqueous phase, which was only second to that of controlling TSO_4^{2-}.

2.3.3. *Clear difference among the response to the reduction in TMg^{2+}, TK^+, and TCa^{2+} concentrations*

Among aerosol components, Mg^{2+}, K^+, and Ca^{2+} had relatively low concentrations (Table 2), and the changes of IAM and aerosol pH under corresponding sensitive tests were relatively small, with slopes of -1.78, -0.41, 1.08, and -0.16, -0.07, -0.35, respectively (Fig. 3). After controlling TMg^{2+} and TK^+, the inorganic aerosol responses had a similar gas-particle conversion mechanism. As shown in Fig. 4(f and g), TMg^{2+} or TK^+ was mainly in the chemical forms of $MgCl_2$ and $Mg(NO_3)_2$ or KCl and KNO_3 in the aerosol aqueous phase. Hence, as the TMg^{2+} or TK^+ concentration was reduced, most of the Cl^- and NO_3^- that had combined with these reduced Mg^{2+} or K^+ could be released directly into the atmosphere, resulting in decreased Cl^- and NO_3^- in the aerosol aqueous phase and increased HCl and HNO_3 in the gas phase. A small part of these Cl^- and NO_3^- concentrations could be combined with NH_4^+, which was transformed from gaseous NH_3. In addition, the concentrations of the ALWC decreased slightly under the comprehensive influence of these responsive species, finally resulting in the linear decrease of the IAM and aerosol pH.

As opposed to controlling TMg^{2+} and TK^+, reducing the TCa^{2+} concentration brought the increase of aerosol loading in the atmosphere (Fig. 3(a)). As shown in Fig. 4(h), after controlling TCa^{2+}, $CaSO_4$ in the aerosol solid phase decreased linearly, but the SO_4^{2-} that had combined with Ca^{2+} in the aerosol solid phase could transfer into the aerosol aqueous phase. Subsequently, a part of the increased SO_4^{2-} in aerosol aqueous phase was combined with the NH_4^+, which was transformed from gaseous NH_3, while another part was abstracted NH_4^+ from existing NH_4Cl and NH_4NO_3 in the aerosol aqueous phase; then Cl^- and NO_3^- were released simultaneously into the gas phase. Moreover, the concentration of the ALWC increased linearly with a slope of 1.67, which was similar to the variation of SO_4^{2-} in the aerosol aqueous phase. Finally, after controlling TCa^{2+}, the IAM and aerosol acidity were all higher than that in base case, revealing that the appropriate presence of TCa^{2+} in the atmosphere has positive effect on the environment in Kitakyushu, Japan, and this was deeply related to the transfer process of SO_4^{2-} between the aerosol solid phase and the aerosol aqueous phase.

2.3.4. *The characteristics of ALWC*

During the gas-particle conversion processes of seven sensitive tests (Fig. 4), the ALWC was basically the most sensitive aerosol component. To further investigate the comprehensive influence of related species on the variation of the ALWC, multiple regression analysis (MRA) was performed by SPSS with a forward method (Tan et al., 2016; Wang et al., 2019; Zhang et al., 2021b). Considering significance levels (*t*-value and *p*-value) and the variance inflation factor (VIF) of each species in the gas and aerosol phases, only six species were the driving factors of the ALWC, as shown in Table 3. The relationship between the concentration variations of the ALWC and the driving factors could be described as follows:

$$\begin{aligned}[ALWC] = {} & 0.01 + 1.68\left[NO_3^-\right] + 5.23\left[Cl^-\right] + 1.83\left[SO_4^{2-}\right] \\ & + 2.81\left[HSO_4^-\right] + 0.34\left[HNO_3\right] \\ & + 0.57\left[NH_3\right]\left(R^2 = 0.99,\ P < 0.05\right),\end{aligned}$$

where [x] represents the concentration decreasing amount (μg/m^3) of each species simulated by the ISORROPIA II model. This equation revealed that the variation of Cl^- with a coefficient value of 5.23 ($p < 0.05$) made the largest contribution to the concentration variations of the ALWC in seven sensitive tests. Meng et al. (2021) and Wen et al. (2021) showed that the ALWC was influenced by secondary aerosols. Huang et al. (2021) clearly demonstrated the positive correlation relationship between ALWC and inorganic nitrate. These researches agreed with our results, while few studies have investigated the influence of Cl^-. In this study, the high coefficient of Cl^- (5.23) proved the key role of sea salts on the concentration variation of the ALWC. Our actual field observations were also consistent with and strongly support the simulation results. Specifically, based on the relationship between the relative humidity and the ALWC in the actual atmospheric conditions (Fig. 2(a)), the data points can be divided into five groups according to the concentration level of TNaCl (Fig. 2(b)). The concentration of the ALWC associated with the lower concentration of sea salts was much smaller than that associated

Table 3 – Multiple regression results.

Model 1		Unstandardized Coefficients		Standardized Coefficients	t-value	p-value	VIF
Response variable	Independent factors	β	Std. Error	Beta			
ALWC	Constant	0.01	0.01	–	0.79	0.43	
	NO_3^-	1.68	0.05	0.91	32.02	0.00	4.00
	Cl^-	5.23	0.11	0.87	45.95	0.00	1.80
	SO_4^{2-}	1.83	0.06	0.66	31.86	0.00	2.16
	HSO_4^-	2.81	0.10	0.57	27.64	0.00	2.15
	HNO_3	0.34	0.05	0.17	6.55	0.00	3.48
	NH_3	0.57	0.10	0.12	5.62	0.00	2.33

with higher one at any RH, further proving the significant influence of sea salts on the concentration of the ALWC of inorganic aerosols.

3. Conclusions

Based on year-round field observations by the filter-pack method and sensitive tests using the ISORROPIR II model, the particle response and inner mechanism with the reduction of the seven species were investigated. The major conclusions are summarized as follows:

- The ALWC made the greatest contribution to the variations of the IAM for five control species (TNaCl, TNH_4^+, TNO_3^-, TMg^{2+}, and TCa^{2+}) except two (TSO_4^{2-} and TK^+) among seven species, and the ALWC in inorganic aerosols was significantly restrained by sea salts.
- The process of converting nitrate and ammonium from the gas phase to the aerosol phase could be enhanced effectively under extremely low concentration level of marine aerosols in the atmosphere.
- IAM could not continue to decrease even though SO_4^{2-} concentration was reduced when the CRR was larger than 60%, mainly being offset by the increase of ALWC.
- The appropriate presence of TCa^{2+} in the atmosphere proved to be useful for the decrease particle concentration and acidity, and this was deeply related to the transfer process of SO_4^{2-} between the aerosol solid phase and the aerosol aqueous phase.

Totally speaking, the present study clearly demonstrated the gas-particle conversion process in seven sensitive tests, and deeply investigated the characteristics of aerosol components in the suburbs of Kitakyushu, Japan, which provides scientific ideas for explaining complex aerosol behaviors in real atmospheric condition. From two perspectives of aerosol pH and mass concentration, limiting the concentration of TSO_4^{2-} or TNO_3^- was the relatively effective and realistic method of mitigating particle pollution in Kitakyushu, Japan. Wang et al. (2020) have proved that the decreased concentration of SO_2 and NO_2 could explain a large fraction of the decreased $PM_{2.5}$ concentrations in China based on the long-term field observation data. Hence, in future works, the accurate inventory of sulfur and nitrogen emissions in Kitakyushu, Japan, and the particle responses under simultaneous reductions of TSO_4^{2-} and TNO_3^- are worth in-depth investigating.

Declaration of Competing Interest

The authors declare that they have no known competing financial interests or personal relationships that could have appeared to influence the work reported in this paper.

REFERENCES

Aikawa, M., Hiraki, T., Horie, Y., Nakatsubo, R., Matsumura, C., Mukai, H., 2017a. Trans-boundary and in-country transport of air pollutants observed in Kobe, Japan by high frequent filter pack sampling method. J. Atmos. Chem. 74, 505–518.

Aikawa, M., Hiraki, T., Tamaki, M., 2005. Characteristics in concentration of chemical species in ambient air based on three-year monitoring by filter pack method. Water Air Soil Pollut. 161, 335–352.

Aikawa, M., Hiraki, T., Tomoyose, N., Ohizumi, T., Noguchi, I., Murano, K., et al., 2013. Local emission of primary air pollutants and its contribution to wet deposition and concentrations of aerosols and gases in ambient air in Japan. Atmos. Environ. 79, 317–323.

Aikawa, M., Hirokawa, K., Murakami, T., 2017b. Daily observation of gas/aerosol by FP method in western part of Japan. In: Proceedings of the 58th Annual Meeting of the Japan Society for Atmospheric Environment, Hyogo, Japan, 6–8 September 2017, p. 454.

Aikawa, M., Morino, Y., Kajino, M., Hiraki, T., Horie, Y., Nakatsubo, R., et al., 2016. Candidates to provide a specific concentration difference for ambient sulfur and nitrogen compounds near the coastal and roadside sites of Japan. Water Air Soil Pollut. 227.

Aikawa, M., Ohara, T., Hiraki, T., Oishi, O., Tsuji, A., Yamagami, M., et al., 2010. Significant geographic gradients in particulate sulfate over Japan determined from multiple-site measurements and a chemical transport model: Impacts of transboundary pollution from the Asian continent. Atmos. Environ. 44, 381–391.

Aikawa, M., Suzuki, M., Murakami, T., Hirokawa, K., 2018. Daily observation of gas/aerosol by FP method in western part of Japan (2). In: Proceedings of the 59th Annual Meeting of the

Japan Society for Atmospheric Environment, Fukuoka, Japan, 12–14 September 2018, p. 245.
Ansari, A.S., Pandis, S.N., 1998. Response of inorganic PM to precursor concentrations. Environ. Sci. Technol. 32, 2706–2714.
Boreddy, S.K., Kawamura, K., 2016. Hygroscopic growth of water-soluble matter extracted from remote marine aerosols over the western North Pacific: Influence of pollutants transported from East Asia. Sci. Total Environ. 557-558, 285–295.
Carnevale, C., Finzi, G., Pisoni, E., Thunis, P., Volta, M., 2012. The impact of thermodynamic module in the CTM performances. Atmos. Environ. 61, 652–660.
Chen, D., Zhao, N., Lang, J., Zhou, Y., Wang, X., Li, Y., et al., 2018. Contribution of ship emissions to the concentration of $PM_{2.5}$: a comprehensive study using AIS data and WRF/Chem model in Bohai Rim Region, China. Sci. Total Environ. 610-611, 1476–1486.
Chen, W., Tang, H., Zhao, H., 2016. Urban air quality evaluations under two versions of the national ambient air quality standards of China. Atmos. Pollut. Res. 7, 49–57.
Fong, B.N., Kennon, J.T., Ali, H.M., 2016. Mole ratio dependence of the mutual deliquescence relative humidity of aqueous salts of atmospheric importance. J. Phys. Chem. A. 120, 3596–3601.
Fountoukis, C., Nenes, A., 2007. ISORROPIA II: a computationally efficient thermodynamic equilibrium model for K^+–Ca^{2+}–Mg^{2+}–NH_4^+–Na^+–SO_4^{2-}–NO_3^-–Cl^-–H_2O aerosols. Atmos. Chem. Phys. 7, 4639–4659.
Gao, J., Wei, Y., Shi, G., Yu, H., Zhang, Z., Song, S., Wang, W., Liang, D., Feng, Y., 2020. Roles of RH, aerosol pH and sources in concentrations of secondary inorganic aerosols, during different pollution periods. Atmos. Environ. 241, 117770.
Ge, X., He, Y., Sun, Y., Xu, J., Wang, J., Shen, Y., Chen, M., 2017. Characteristics and formation mechanisms of fine particulate nitrate in typical urban areas in China. Atmosphere 8, 62.
He, Y., Gu, Z., Lu, W., Zhang, L., Okuda, T., Fujioka, K., et al., 2019. Atmospheric humidity and particle charging state on agglomeration of aerosol particles. Atmos. Environ. 197, 141–149.
Huang, W., Yang, Y., Wang, Y., Gao, W., Li, H., Zhang, Y., et al., 2021. Exploring the inorganic and organic nitrate aerosol formation regimes at a suburban site on the North China Plain. Sci. Total Environ. 768, 144538.
Karydis, V.A., Tsimpidi, A.P., Fountoukis, C., Nenes, A., Zavala, M., Lei, W., et al., 2010. Simulating the fine and coarse inorganic particulate matter concentrations in a polluted megacity. Atmos. Environ. 44, 608–620.
Khan, M.F., Hirano, K., Masunaga, S., 2010. Quantifying the sources of hazardous elements of suspended particulate matter aerosol collected in Yokohama, Japan. Atmos. Environ. 44, 2646–2657.
Kong, L., Du, C., Zhanzakova, A., Cheng, T., Yang, X., Wang, L., et al., 2018. Trends in heterogeneous aqueous reaction in continuous haze episodes in suburban Shanghai: an in-depth case study. Sci. Total Environ. 634, 1192–1204.
Li, X., Zhang, Q., Zhang, Y., Zhang, L., Wang, Y., Zhang, Q., Li, M., Zheng, Y., Geng, G., Wallington, T.J., Han, W., Shen, W., He, K., 2017a. Attribution of $PM_{2.5}$ exposure in Beijing–Tianjin–Hebei region to emissions: implication to control strategies. Sci. Bull. 62, 957–964.
Li, X., Zhang, Q., Zhang, Y., Zheng, B., Wang, K., Chen, Y., et al., 2015. Source contributions of urban $PM_{2.5}$ in the Beijing–Tianjin–Hebei region: changes between 2006 and 2013 and relative impacts of emissions and meteorology. Atmos. Environ. 123, 229–239.
Li, Y.J., Liu, P.F., Bergoend, C., Bateman, A.P., Martin, S.T., 2017b. Rebounding hygroscopic inorganic aerosol particles: liquids, gels, and hydrates. Aerosol Sci. Technol. 51, 388–396.
Meng, J., Li, Z., Zhou, R., Chen, M., Li, Y., Yi, Y., et al., 2021. Enhanced photochemical formation of secondary organic aerosols during the COVID-19 lockdown in Northern China. Sci. Total Environ. 758, 143709.
Ng, C.F.S., Hashizume, M., Obase, Y., Doi, M., Tamura, K., Tomari, S., et al., 2019. Associations of chemical composition and sources of $PM_{2.5}$ with lung function of severe asthmatic adults in a low air pollution environment of urban Nagasaki, Japan. Environ. Pollut. 252, 599–606.
Quan, J., Zhang, X., 2008. Assessing the role of ammonia in sulfur transformation and deposition in China. Atmos. Res. 88, 78–88.
Roberts, G., Wooster, M.J., 2021. Global impact of landscape fire emissions on surface level $PM_{2.5}$ concentrations, air quality exposure and population mortality. Atmos. Environ. 252, 118210.
Roig Rodelas, R., Perdrix, E., Herbin, B., Riffault, V., 2019. Characterization and variability of inorganic aerosols and their gaseous precursors at a suburban site in northern France over one year (2015–2016). Atmos. Environ. 200, 142–157.
San Martini, F.M., West, J.J., de Foy, B., Molina, L.T., Molina, M.J., Sosa, G., et al., 2005. Modeling inorganic aerosols and their response to changes in precursor concentration in Mexico City. J. Air Waste Manage. Assoc. 55, 803–815.
Song, Q., Osada, K., 2021. Direct measurement of aerosol acidity using pH testing paper and hygroscopic equilibrium under high relative humidity. Atmos. Environ. 261, 118605.
Sudheer, A.K., Rengarajan, R., 2015. Time-resolved inorganic chemical composition of fine aerosol and associated precursor gases over an urban environment in western India: Gas-aerosol equilibrium characteristics. Atmos. Environ. 109, 217–227.
Sun, Y., Wang, Z., Wild, O., Xu, W., Chen, C., Fu, P., et al., 2016. APEC Blue": secondary aerosol reductions from emission controls in Beijing. Sci. Rep. 6, 20668.
Tan, H., Cai, M., Fan, Q., Liu, L., Li, F., Chan, P.W., et al., 2017. An analysis of aerosol liquid water content and related impact factors in Pearl River Delta. Sci. Total Environ. 579, 1822–1830.
Tan, K.C., San Lim, H., Jafri, M.Z.M., 2016. Prediction of column ozone concentrations using multiple regression analysis and principal component analysis techniques: A case study in peninsular Malaysia. Atmos. Pollut. Res. 7, 533–546.
Walker, J.T., Robarge, W.P., Shendrikar, A., Kimball, H., 2006. Inorganic $PM_{2.5}$ at a U.S. agricultural site. Environ. Pollut. 139, 258–271.
Wang, H., Ding, J., Xu, J., Wen, J., Han, J., Wang, K., et al., 2019. Aerosols in an arid environment: The role of aerosol water content, particulate acidity, precursors, and relative humidity on secondary inorganic aerosols. Sci. Total Environ. 646, 564–572.
Wang, J., Zhang, X., Zhang, K., Zheng, Z., 2018. Characterization of size distribution and concentration of atmospheric particles during summer in Zhuzhou, China. Pol. J. Environ. Stud. 27, 2793–2800.
Wang, Y., Gao, W., Wang, S., Song, T., Gong, Z., Ji, D., et al., 2020. Contrasting trends of $PM_{2.5}$ and surface-ozone concentrations in China from 2013 to 2017. Natl. Sci. Rev. 7, 1331–1339.
Wen, Z., Xu, W., Pan, X., Han, M., Wang, C., Benedict, K., et al., 2021. Effects of reactive nitrogen gases on the aerosol formation in Beijing from late autumn to early spring. Environ. Res. Lett. 16, 025005.
Wu, Z., Wang, Y., Tan, T., Zhu, Y., Li, M., Shang, D., et al., 2018. Aerosol liquid water driven by anthropogenic inorganic salts: implying its key role in haze formation over the North China Plain. Environ. Sci. Technol. Lett. 5, 160–166.
Xu, L., Duan, F., He, K., Ma, Y., Zhu, L., Zheng, Y., et al., 2017. Characteristics of the secondary water-soluble ions in a typical autumn haze in Beijing. Environ. Pollut. 227, 296–305.

Xu, Z., Liu, M., Zhang, M., Song, Y., Wang, S., Zhang, L., et al., 2019. High efficiency of livestock ammonia emission controls in alleviating particulate nitrate during a severe winter haze episode in northern China. Atmos. Chem. Phys. 19, 5605–5613.

Xue, M., Ma, J., Yan, P., Pan, X., 2011. Impacts of pollution and dust aerosols on the atmospheric optical properties over a polluted rural area near Beijing city. Atmos. Res. 101, 835–843.

Yin, S., Huang, Z., Zheng, J., Huang, X., Chen, D., Tan, H., 2018. Characteristics of inorganic aerosol formation over ammonia-poor and ammonia-rich areas in the Pearl River Delta region, China. Atmos. Environ. 177, 120–131.

Zhang, X., Eto, Y., Aikawa, M., 2021a. Risk assessment and management of $PM_{2.5}$-bound heavy metals in the urban area of Kitakyushu, Japan. Sci. Total Environ. 795, 148748.

Zhang, X., Murakami, T., Wang, J., Aikawa, M., 2021b. Sources, species and secondary formation of atmospheric aerosols and gaseous precursors in the suburb of Kitakyushu, Japan. Sci. Total Environ. 763, 143001.

Zhang, X., Wang, J., Zhang, K., Shang, X., Aikawa, M., Zhou, G., et al., 2022. Year-round observation of atmospheric inorganic aerosols in urban Beijing: Size distribution, source analysis, and reduction mechanism. J. Environ. Sci. 114, 354–364.

Zhang, X., Zhang, K., Liu, H., Lv, W., Aikawa, M., Liu, B., et al., 2020. Pollution sources of atmospheric fine particles and secondary aerosol characteristics in Beijing. J. Environ. Sci. 95, 91–98.

Zhang, X., Zhang, K., Lv, W., Liu, B., Aikawa, M., Wang, J., 2019. Characteristics and risk assessments of heavy metals in fine and coarse particles in an industrial area of central China. Ecotoxicol. Environ. Saf. 179, 1–8.

Zhang, Z., Wang, W., Cheng, M., Liu, S., Xu, J., He, Y., et al., 2017. The contribution of residential coal combustion to $PM_{2.5}$ pollution over China's Beijing-Tianjin-Hebei region in winter. Atmos. Environ. 159, 147–161.